Preventive Coating of Tri-calcium Phosphate (TCP) on Implantable 304L SS

Priyanka Majee[1], P. K. Mitra[2], P. Basak[3]

[1]*Metallurgical and Material Engineering Department, Jadavpur University*

[2] *Metallurgical and Material Engineering Department, Jadavpur University*

[3] *School of Bio-science and Engineering , Jadavpur University*

Corresponding Author.E-mail- priyankamajee11@gmail.com

Abstract

The present study explores beta tri-calcium phosphate (β-TCP) coating with nano-metric grain on AISI grade 304L stainless steel (304L SS) by voltage- and current-assisted EPD technique for developing orthopedic implants with improved corrosion resistance properties. After coating, XRD, SEM, EDX, and TEM techniques were used to systematically examine the quality and nature of the coatings. Potentiodynamic polarization tests and electrochemical impedance spectroscopy (EIS) in Ringer's solution were carried out with the coated samples to assess respectively corrosion resistance and surface behavior. The results show that brushite + calcite rather than β-TCP formed by the process, and the grain sizes were in nano-metric range; also, current assisted EPD coating gave better corrosion resistance compared to voltage assisted EPD coating, and so would prove superior for implant purposes.

Keywords: Coated implants, TCP coating, EPD technique, 304L SS, Corrosion tests

1.Introduction

Low carbon versions of AISI grade 304 and 316 stainless steels (respectively 304L SS and 316L SS) are extensively used for many years as bio-implant materials because of their bio-compatibility (i.e., non-allergic or other adverse medical reactions), corrosion resistance in body fluids, good mechanical properties, combined with reasonable cost, cf. [1-2].. However, the corrosion problem, and leaching out of solute ions, is serious with such implants after prolonged exposure [3-14]. The leaching out of solute ions reduce biocompatibility (hexavalent Cr is a carcinogen), and degradation of mechanical properties. Localized corrosion is the root cause of failures of implantable stainless steel.

Application of bio-ceramic coating, namely hydroxyapatite (HAp) or tri-calcium phosphate (TCP), on the implant material was thought of as solution - similarity with body bone cells with the coating material should also promote bone cell formation. β-TCP is stable at room temperature [15, 16], and the β–α transformation takes place at 1125^{o} C [16, 17]. β- TCP is component of several mono- or biphasic bio-ceramic composites. A of literature is good amount available on HAp coating on stainless steels cf. [18, 19]. In comparison, lesser number of studies is concerned with β-TCP, cf. [20]. β-TCP, with a similar mineral phase of natural bone tissue, has been extensively studied and clinically used for bone regeneration because of superior bio-compatibility, and promoting osteo-integration [21 ,22, 23], and is attractive as a coating material. However compared to HAp, β-TCP is less well studied as a coating material for bio-implants.

Various coating methods attempted are, physical vapour deposition (PVD), chemical vapour deposition (CVD), plasma spraying, dip coating, and electrophoretic deposition (EPD) with varying degrees of success. The relevant points for the quality of coating are bonding with substrate, thickness of coating,

uniformity of coating, porosity of coating, and the complexity of the substrate geometry. Out of these various coating methods, EPD appears very promising [19, 21]. In EPD, particles suspended in a liquid medium are forced to migrate towards an electrode under the effect of an external electric field applied to the suspension (electrophoresis), where they form a relatively compact film. Its advantages are: the coating formed is dense and homogeneous, it can be used with substrates of rather complex geometry, it has high versatility with respect to the coating material, nanometric grain sized coatings are possible, and the process requires simple apparatus set-up which makes it cost effective. However the reports on applying EPD method for bio-ceramic coatings on implant materials are relatively less: reference [18, 19] report HAp coating on austenitic stainless steels while reference [20] report using EPD for β-TCP-chitosan coating of stainless steels. The results from these studies were considered satisfactory. It may be noted that these studies used voltage assisted EPD coating; the other possibility, namely using current assisted EPD does not seem to have been explored in the literature.

In the present study an attempt has been made to deposit β- TCP on 304 L SS by generating it in-situ in the EPD cell by chemical reaction with a view to restricting the grain size of the deposited grains to nanometric ranges. If the coated material grain size is restricted to nano-metric ranges, it may be anticipated that, apart from better mechanical properties for the coating, a coat with adequate surface roughness to promote cell adhesion and cell growth, yet free of inter-connected pores which severely degrade the corrosion resistance of the implant. This aspect however does not seem to have been addressed in the literature. Also, both voltage and current assisted EPD techniques were used. Coating obtained was followed up by detailed characterization studies using XRD, SEM, EDX, TEM, as well as corrosion tests.

2. Materials and methods

Table 1 lists the types of samples prepared and the characterization methods adopted in each case.

Table 1. Overview of type of samples and experiments.(**x** are not performed)

Type of Sample		Sample Number	Type of Experiments				
			XRD	SEM	EDX	TEM	Corrosion Tests
Synthesized TCP		1	√	**x**	**x**	√	**x**
Voltage assisted EPD (fixed current)	20 V, 1 h	2	**x**	√	√	**x**	√
	20 V, 20 min	3	√	√	√	√	√
Current assisted EPD (fixed voltage)	30 mA, 1 h	4	√	√	√	√	√

2.1 EPD Coating of 304L SS

Three samples of 304L SS (25 mm length x 10 mm width x 5 mm thickness) were taken to carry out all the experiments. The samples were mechanically polished following standard procedures down to 2/0 grade emery sheets. Surface roughness of very fine scale is expected to improve adhesion between the base material and the coating. These were then washed by sonicating in acetone solution for 20 min.

The stainless steel samples were then coated using the EPD [5] technique. For this purpose, 100 ml of double distilled water was taken in a mechanically stirred bath. Then, AR grade $CaCO_3$ powder was added to the bath so as to obtain a 1 M solution. The bath was then slowly heated to 80^0 C, which was maintained for the subsequent steps. Then two electrodes were immersed in the bath; the polished 304L SS specimen, wrapped with Teflon tape so as to expose only the 10 mm x 5 mm side to the solution was connected to the negative terminal of the EPD unit, so that once the dc circuit was put on, it would form the cathode. An uncoated 304L SS piece of similar dimensions, but without Teflon wrapping (so as to expose a much larger surface to the electrolyte bath) was connected to the positive terminal of the EPD unit. Next, 0.6 M H_3PO_4 solution in double distilled water added drop by drop to this solution. This was aimed to produces in-situ β−TCP by the following chemical reaction:

$$3CaCO_3\,(1M) + 2H_3PO_4\,(0.6M) = Ca_3(PO_4)_2\,(TCP) + 3H_2O + 3CO_2$$

After the reaction progressed for a few minutes, the EPD unit was turned. The rate of addition of the H_3PO_4 solution was adjusted such that by the time the EPD campaign completed, the volume of total phosphate solution added was 100 ml, the stoichiometric amount needed for complete reaction of the $CaCO_3$ used. Electrophoretic deposition parameters for the experiment were constant current [5] or constant voltage [6], with the duration of EPD fixed independently. Both these control methods were tried because it was not known *a priori* which of these would produce better coatings. These parameters are recorded in Table 1. After coating, the sample was baked at 80-90º C for 1 hour. Characterization of the coated samples was carried out after that. Figure 1 shows the photographs of typical surface before coating, and after coating and baking.

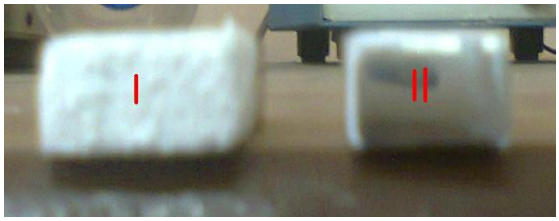

Figure 1: Photographs of coated surface of sample no 4 after baking (I), and polished surface prior to coating (II). Coating results in slightly uneven surface with pure white colour.

2.2 Preparation of Synthesized TCP Sample

The same procedure was followed to synthesize TCP, except that the electrodes and the EPD unit were not used. In this case, after the completion of the addition of H_3PO_4 drops, the solution was allowed to rest at least 1 h. The $Ca_3(PO_4)_2$ precipitate was then filtered out, and dried at 90^0 C for 2-3 h. The dried $Ca_3(PO_4)_2$ powder was then mortared to obtain fine powder.

2.3 Corrosion Testing

A Gamry 600^{TM} potentiostat, a standard three electrode corrosion cell consisting of a calomel reference electrode, a graphite rod as a counter electrode and the specimen to be tested as the working electrode were used for the corrosion tests. Of the solutions considered as standard for testing implant materials, Ringer's solution (NaCl: 8.6 g/l, KCl: 0.6 g/l and $CaCl_2$: 0.66 g/l) was chosen for the present study. Polarization experiments with scan rate of 1 mV/s were carried out as per ASTM ST72. The corrosion current (I_{corr}) and the corrosion potential (E_{corr}) values were obtained by Tafel's extrapolation method.

Electrochemical impedance spectroscopy (EIS) was carried out with the same equipment in the frequency range of .01 Hz to 300 kHz. The r m s value of the applied alternating signal was 0.01 V. The software generated the Bode plots, (i.e., the frequency response of the system in terms of the plots of magnitude of the frequency response, and the phase shift), and the Nyquist plots (plot of the imaginary part of the impedance against the real part). The software permitted analyzing these plots in terms of various models; by trial and error, the CPE with diffusion model appeared to best correlate the data. The software yielded the values of the corresponding parameters, determined using the simplex algorithm.

2.4 Other Characterization Methods

X-Ray Diffraction analysis: Phase identification and crystalinity of the samples were carried out using Miniflex model diffractometer from Rigaku Co., Tokyo, Japan at ambient temperature. Monochromatic Cu Kα X ray radiation (wavelength = 0.154059 nm) in the step scanning mode was used. Tube voltage was 30 kV and the tube current was 15 mA. The XRD patterns were recorded in the 2θ range of 0-80º with scan speed of 1 deg/min.

***SEM and EDX*:** SEM and EDX characterization was carried out using a JEOL jsm-6360 (Japan) SEM equipped with EDX facility.

***Transmission Electron Microscopy (TEM)*:** TEM study was limited to determining the grain size of powder, the synthesized TCP powder, or TCP powder obtained by scratching the surface of the coated

samples. HRTEM, (JEOL, model no-JEM 2100) was used for this purpose. For this study, a small amount of the powder sample was taken, adequate amount of ethanol was added to this powder, and then the mixture sonicated in an ultrasound sonicator for 1 h. With a micropipette, a few drops of the mixture were dropped on a copper grid, dried, and then desiccated for 24 h. The grid was then inserted in the TEM for study.

3. Results and Discussion

3.1 XRD

The XRD patterns are shown in Fig. 2, and results from comparing the peak positions with data from JCPDS cards are summarized in Table 2. It was found that the XRD pattern of TCP sample no 1 powder matched with that for brushite ($CaHPO_4$). EPD however resulted in formation of monetite ($CaHPO_4$); in addition, calcite ($CaCO_3$) was also formed, which was not detected in the synthesized sample, sample number 1. However, the $CaCO_3$ content was found to be higher for samples coated with varying voltage (e.g., sample no 3) compared to the sample that coated with varying current, sample no 4. It may also be noted that in each case, the TCP became hydrated.

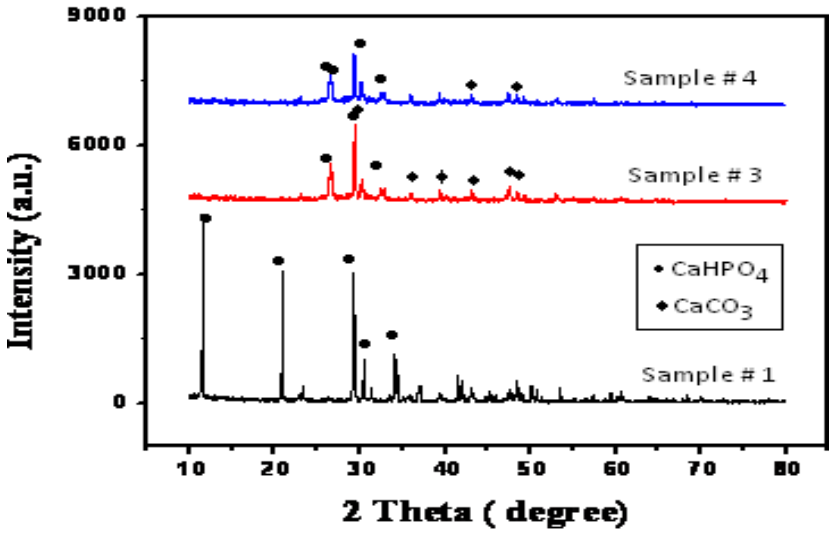

Figure. 2 : XRD patterns for different specimens

Table 2: Comparison of the peak positions in figure 1 with data from JCPDS cards

Sample name	Phase ID	JCPDS card no	d(Å)	2θ	Height % (CPS)
Sample 1	$CaHPO_4$ (Brushite)	01-072-0713	7.5900	11.650	100.0
			4.2372	20.949	79.5
			3.0461	29.296	53.7
			2.9244	30.544	34.9
			2.6454	34.17	32.4
Sample 3	$CaHPO_4$ (Monetite)	01-072-1760	3.3579	26.523	100.0
			2.9586	30.182	44.7
			2.7172	32.937	31.9
	$CaCO_3$ (Calcite)	01-072-1937	3.0387	29.369	100.0
			2.4970	35.936	14.0
			2.2868	39.370	17.7
			2.0963	43.117	14.9
			1.9145	47.449	18.8
			1.8772	48.452	19.5
Sample 4	$CaHPO_4$ (Monetite)	01-070-0360	3.3784	26.360	92.1
			3.3550	26.547	92.5
			2.9530	30.241	100.0
			2.7257	32.832	43.6
	$CaCO_3$ (Calcite)	01-072-1214	2.0942	43.163	14.0
			1.8752	48.507	19.6

3.2 SEM and EDX

SEM micrographs of the coated samples at X1000 magnification, [Figs. 3(a-c)], show that in each case, the coating was continuous, but size and shape of grains varied with the variation of coating conditions, from needle like grains growing in different directions for sample no 4, to grains with aspect ratios closer to 1 for sample nos. 2 and 3. For the last two instances, the grains appear to become better defined with increasing duration of deposition. These images may be compared with those for the synthesized TCP powder, Fig. 3(d), and that for polished bare 304L SS, Fig. 3(e).

The results of EDX are presented in Figs. 4(a-e) and Table 3. For 304L SS, Ca and P peaks were absent, as expected. For synthesized TCP, sample no 1, the Ca/P atomic ratio was 1.49, close to the ideal value of 1.5. For the voltage assisted EPD coatings, the Ca/P atomic ratios were 0.87 for sample no 2 and 1.04 for sample no 3, much smaller than the ideal value of 1.5. In contrast, for the current assisted EPD coating, sample no 4, Ca/P atomic ratio was 1.6, close to but slightly higher than the ideal value. Obviously, EDX fails to detect any hydrogen.

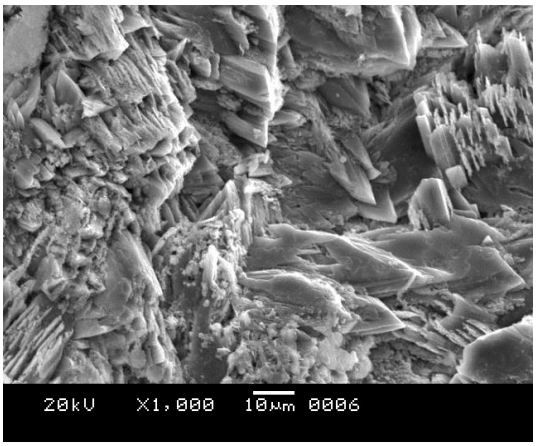

(a) Sample no 4

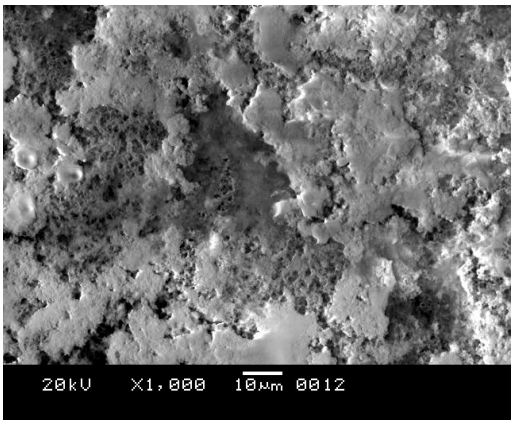

(b) Sample no 3

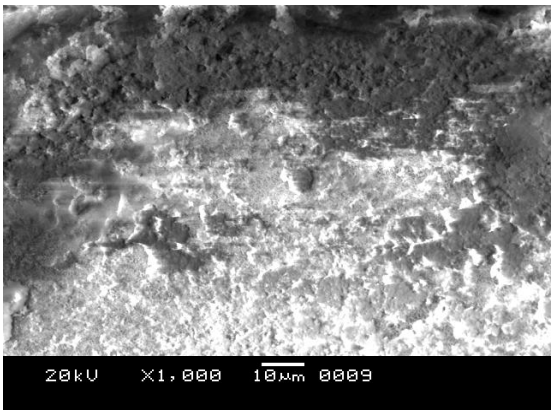

(c) Sample no 2

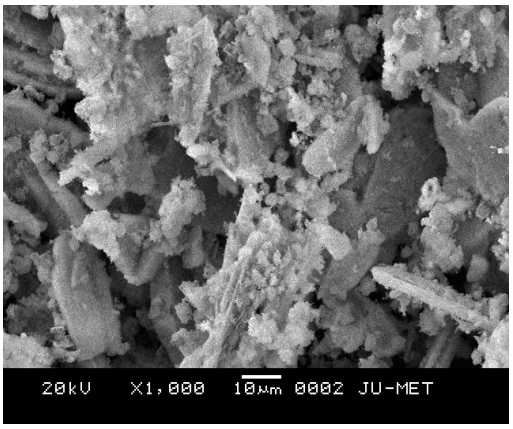

(d) Synthesized TCP

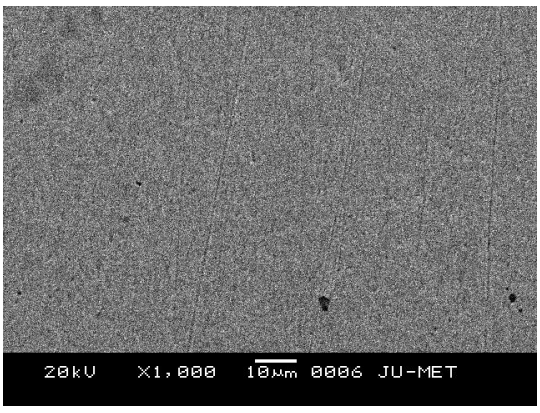

(e) Polished 304 SS sample

Figure 3. SEM micrographs of specimens : (a) Sample no 4; (b) Sample no 3; (c) Sample no 2; (d) Synthesized TCP; (e) Polished 304 SS sample.

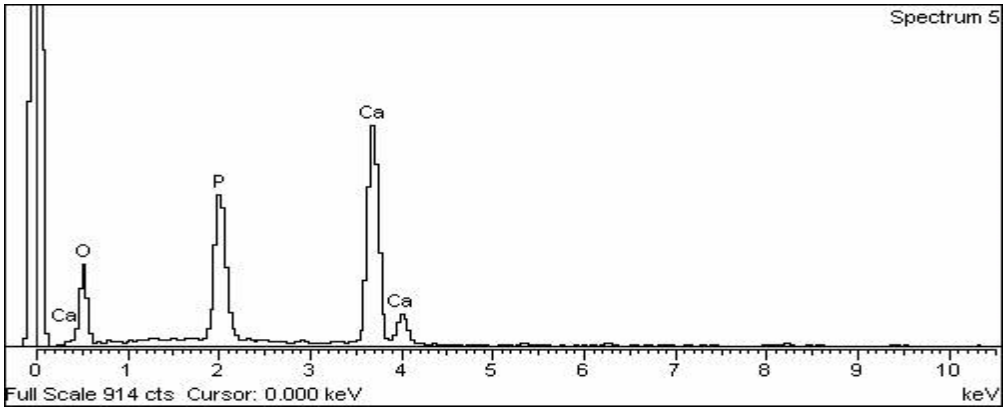

(a) Sample no- 4

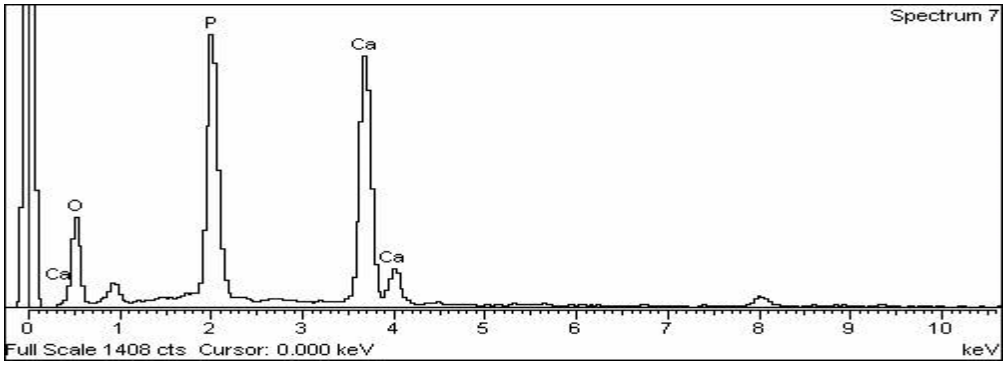

(b) Sample no- 3

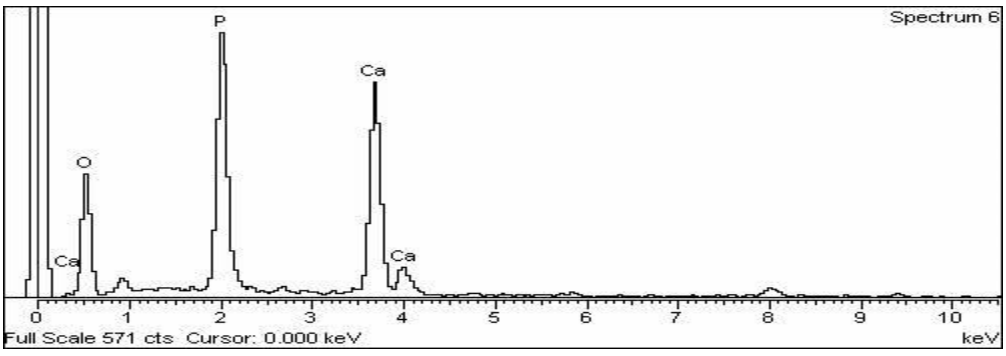

(c) Sample no- 2

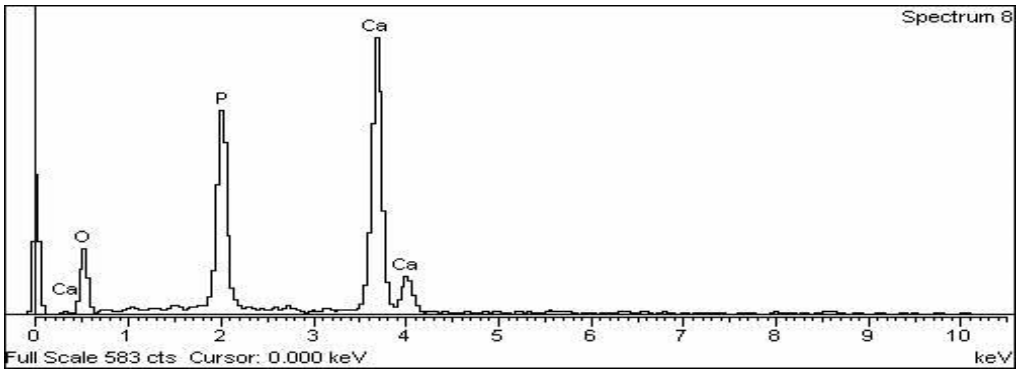

(d) Sample no. 1 (synthesized TCP)

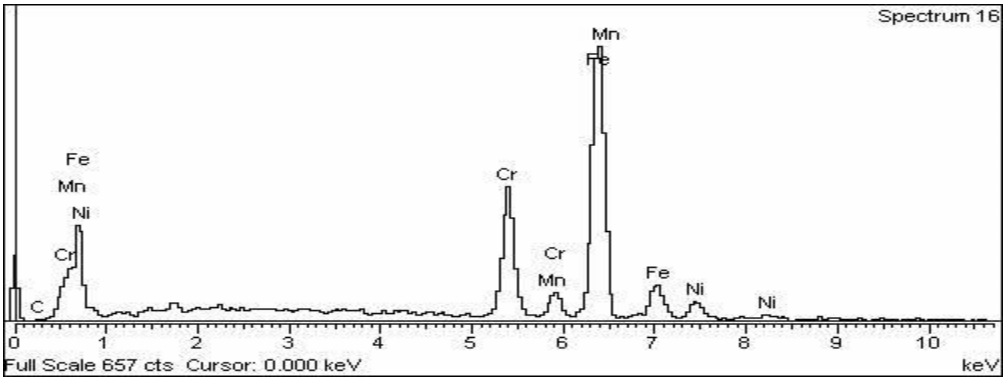

(e) 304L SS polished

Figure 4. EDX micrographs of specimens : (a) Sample no 4; (b) Sample no 3; (c) Sample no 2; (d) Sample no 1 (synthesized TCP); (e) Polished 304 SS sample.

Table 3: EDX data for the substrate material (304L SS) and the other 4 samples

Sample name	Element	Weight %	Atomic %
Substrate material (304L SS)	C	1.22	5.38
	Cr	18.97	19.30
	Mn	3.62	3.48
	Fe	69.60	65.91
	Ni	6.59	5.93
Sample 1 (synthesized TCP)	Ca	35.25	20.11
	P	18.28	13.49
	O	46.47	66.40
Sample 2	Ca	23.24	12.26
	P	20.69	14.06
	O	55.97	73.67
Sample 3	Ca	28.17	15.43
	P	21.14	14.99
	O	50.69	69.58
Sample 4	Ca	30.86	16.56
	P	14.67	10.19
	O	54.47	73.24

3.3 TEM

For sample no 1 (synthesized TCP). Fig. 5(a) shows the lattice image, Fig. 5(b) the microstructure and Fig. 5(c) the selected area electron diffraction pattern. Figures 6(a-c) show the corresponding elaborated results for sample no 3. For sample no 4, Figs. 7(a) and 7(d) show respectively the lattice image and the selected area electron diffraction pattern, while Figs. 7(b-c) show microstructures at two different locations. From the microstructures, the morphology was recorded and also the average grain size determined. The lattice images and the SEAD results were used to compute inter-planar spacings, and hence the reflecting planes. These results are summarized in Table 4.

Table 4. Summary of the TEM results

Sample number	**Average Grain size**	**JCPDS card no**	**Interplanar spacing (d in Å)**	**Diffracting planes (h k l)**	**Morphology**
Sample no 1 (Fig. 5)	20-150 nm	72-0713	3.8059, 3.0501 2.9325	(0 4 0), (0 6 0), (2 3 $\bar{1}$)	Mostly globular with needles, agglomerated
Sample no 3 (Fig. 6)	40-80 nm	72-1937 71-1760	3.3547, 2.7548 2.2151	(0 1 2), (1 1 1), (1 3 $\bar{1}$)	Irregular, Detached
Sample no 4 (Fig.7)	40-80 nm	72-1214 70-0360	3.8700, 2.7555 2.4821	(0 1 2), ($\bar{1}$ 2 0), ($\bar{2}$ 0 2)	Irregular, Detached Colonies

In sample no 1, round, irregular and needle shaped particles 20 - 150 nm in size were observed. (Figs. 5(a)); results from the lattice image and SEAD match with the corresponding XRD results, and the phase can be identified as brushite {JCPDS-72-0713}. In sample no 3, the grains were found to be more uniform in size, and distributed in an irregular manner. From the d-spacings and SEAD, the phases were identified as brushite and $CaCO_3$, in agreement with the corresponding XRD results. In sample no 4, the particles were of uniform size ~ 20 nm, and the phases are identified as brushite and $CaCO_3$. It is apparent that the eletrophoretic deposits are much finer with more uniform distribution.

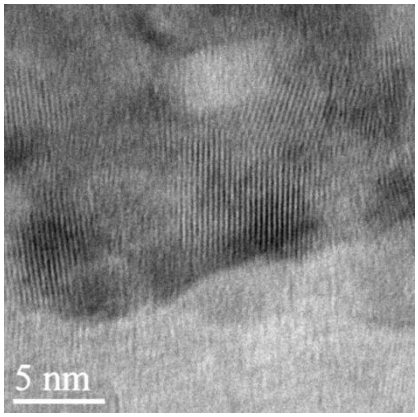

(a)

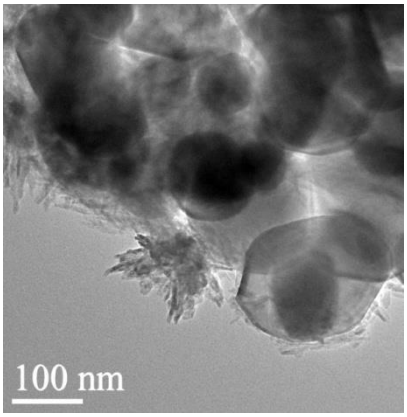

(b)

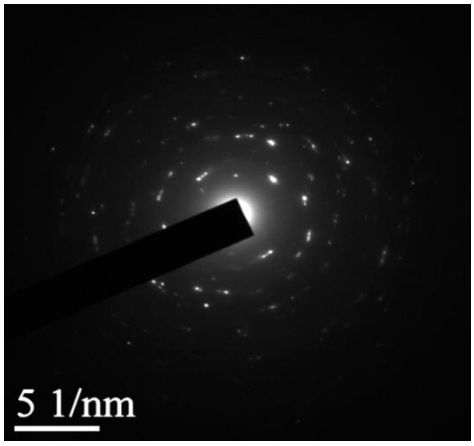

(c)

Figure 5. Sample 1: (a) lattice imaging, (b) microstructure (c) selected area electron diffraction SEAD

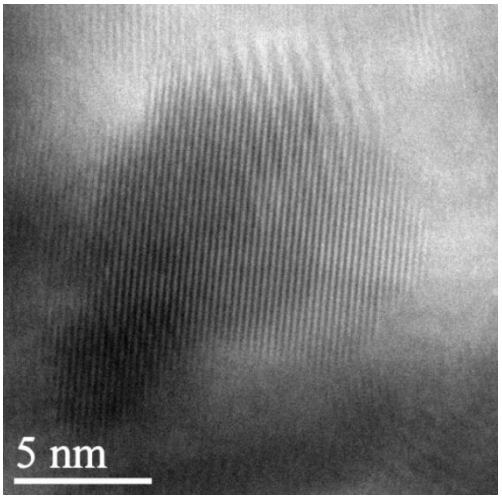

(a)

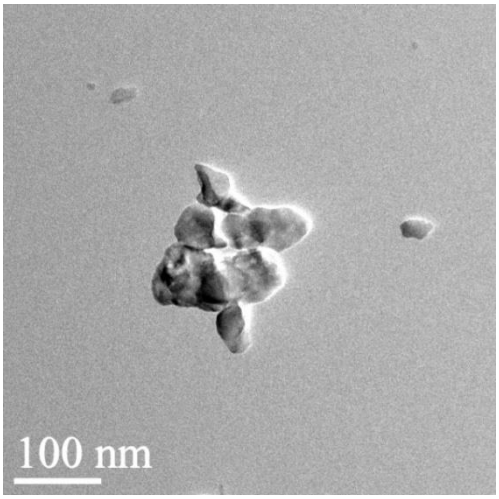

(b)

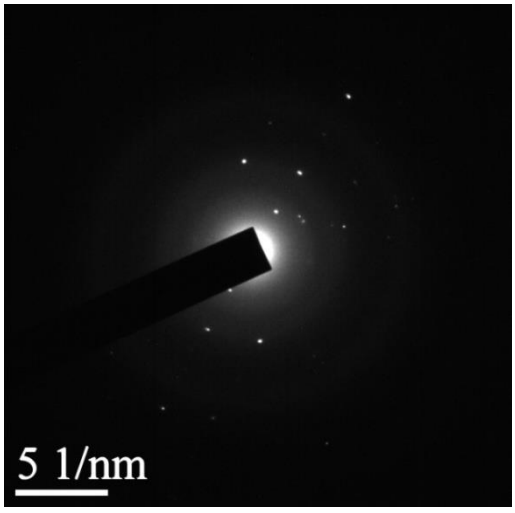

(c)

Figure 6. Sample no 3: (a) lattice imaging, (b) microstructure (c) selected area electron diffraction SEAD

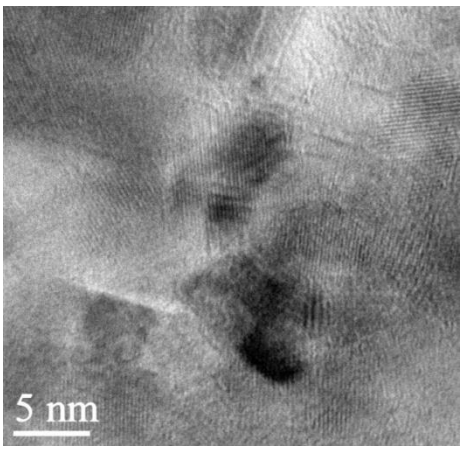

(a)

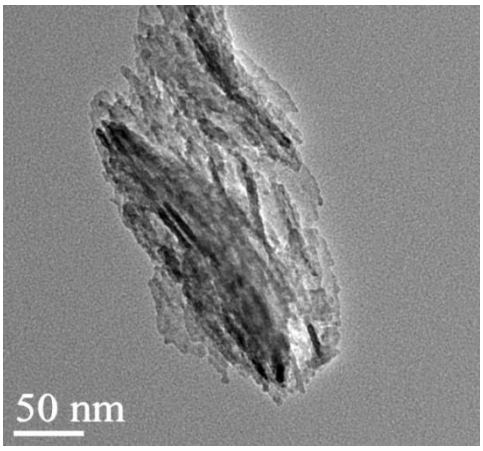

(b)

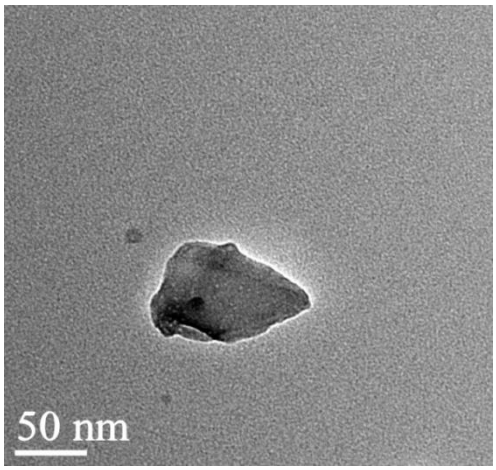

(c)

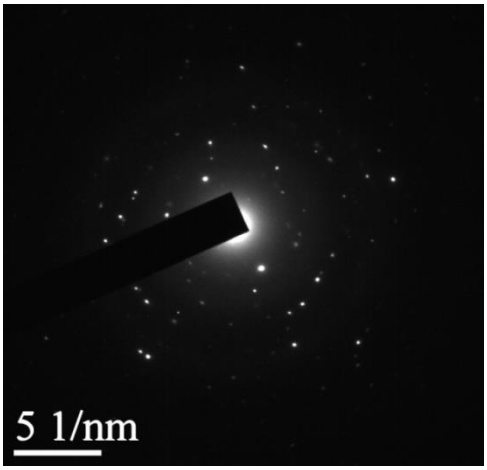

(d)

Figure 7: Sample no 4: (a) Lattice (b) & (c) Microstructure of different side (d) SEAD

3.4 Corrosion Testing

Figure 8 shows the potentio dynamic polarization curves of the three coated samples. The I_{corr} and E_{corr} values were obtained by Tafel's extrapolation method from these curves, and the values are tabulated in Table 3. From Figure 8 and Table 5 it is clear that the sample coated with varying current shows best E_{corr} and I_{corr} value among the three samples.

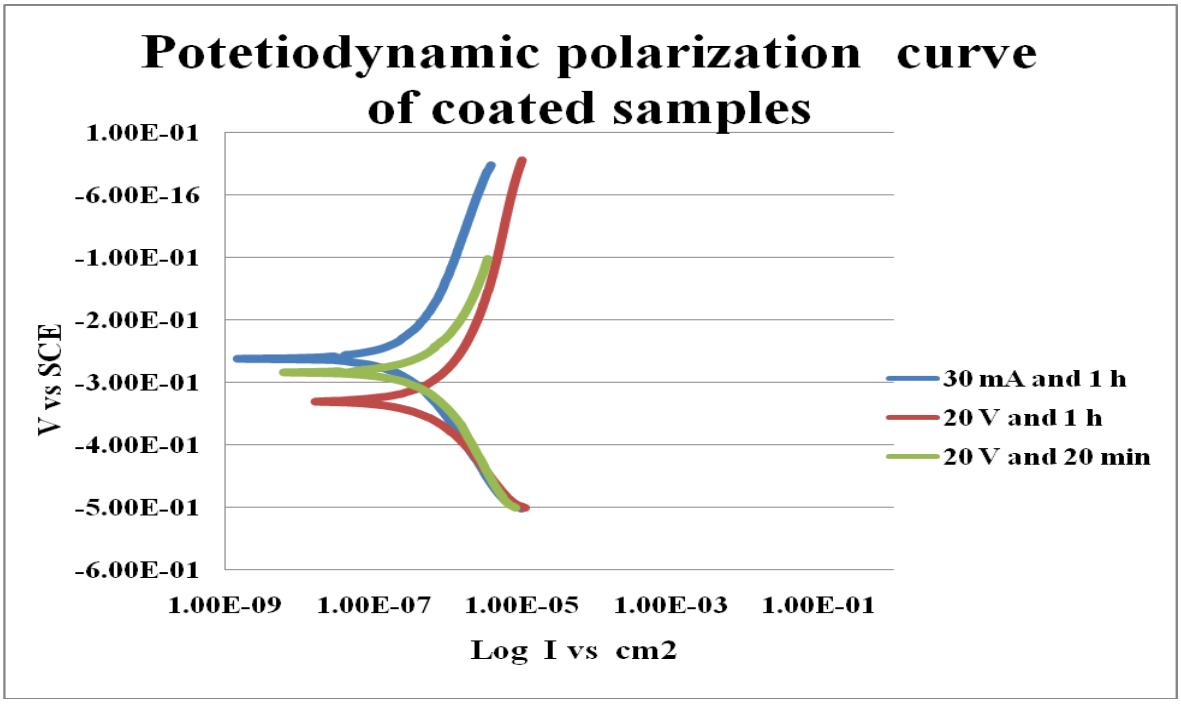

Figure 8. Potentiodynamic polarization curves of coated 304L SS

Table 5: Polarization data

Sample	**I_{corr} (A/cm^2)**	**E_{corr} (mV)**
Sample no- 4	1*E-07	- 262
Sample no- 3	2*E-07	- 284
Sample no- 2	4*E-07	- 331

The data in Table 5 show that E_{corr} value of sample no 4 is nobler than those for the other two coated samples, and as such sample no 4 is more corrosion resistant. However, there was not much variation in I_{corr} values. Possibly, interlocking needle like growth of TCP on surface observed in SEM (Fig. 3(a)) could provide better corrosion barrier.

EIS was used to obtain the Bode plot and Nyquist plots for the three coated samples. Figure 9 shows these plots for sample no 4 as example. All the Bode and Nyquist data are consistent with the model of Constant Phase Element (CPE) with diffusion (see, [24] for one application of this model, and also other references cited therein). In Fig. 9, the dots are the test data, and the solid lines (in the Bode plot, the blue line is for Bode magnitudes, and the red line is for the Bode phase) the templates for the CPE with diffusion model. The equivalent circuit for the CPE with diffusion model is shown in Fig 10. The values reported in Table 6 were calculated after comparing with test data and template data.

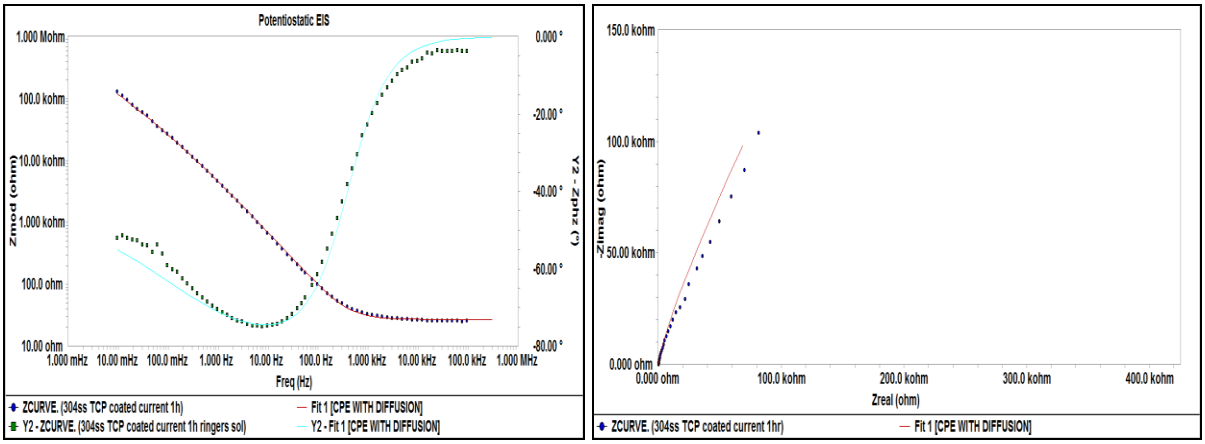

A.Bode plot **B. Nyquist plot**

Figure 9. EIS of sample no 4.

.

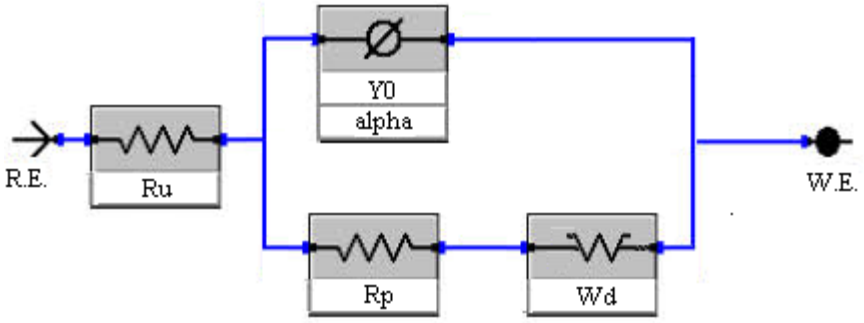

Figure 10: Equivalent circuit for CPE with diffusion

Table 6: EIS results for CPE with diffusion model

Sample	**R_p (ohm-cm^2)**	**R_u (ohm-cm^2)**	**Y_0 (S* s^a)**	**W_d (S* s^(1/2))**
Sample no 4	32.86	26.97	31.46e-6	25.52e-6
Sample no 3	15.61	25.07	33.49e-6	41.59e-6
Sample no 2	45.42	25.59	27.10e-6	15.72e-6

The polarization resistance R_p and the Warburg diffusion W_d are inversely proportional to the corrosion rate, while corrosion rate is directly proportional to solution resistance R_u. Y0 Constant Phase Element is the of the capacitance of the preventive layer. For best corrosion resistance, R_p, and Y_o values should be highest .and R_u should be the lowest. For no single sample in Table 6, this combination is observed, suggesting that all the samples should offer good corrosion resistance. However, sample 4 appears to present an optimum combination. This agrees with the conclusion from the polarization curves.

Conclusion

1. 1.The Ca:P ratio as obtained from EDX for the TCP deposited by current assisted EPD (sample no 4) is close enough to the ideal value.
2. While the SEM image of the coated samples showed continuous coating in all cases, although with different morphologies. XRD patterns showed that CP coating by EPD resulted also in generation of $CaCO_3$.
3. The TEM images indicate that the particle size in all the deposits were in nano-metric range.
4. Potentiodynamic polarization studies showed that while all the coatings gave good corrosion resistance, the best result was obtained for the current assisted coating (sample 4). This corrosion was consistent with EIS results, analyzed with CPE with diffusion model.

5. To summarize, all the coatings proved to be with grains in the desired size range, and yielded corrosion resistant coatings; however, current assisted EPD technique yielded the best results. The deposits however proved to be brushite + calcite, and not exactly β-TCP as targeted. Further studies are necessary to explore the possibility of pure β-TCP coating.

Acknowledgement

We would like to thank the Technical Quality Improvement Programme Phase-II without their funding work is never be possible.

References

1. Disegi JA Eschbach L, *Injury* 2000 Dec:31 Suppl 4:2-6
2. Zitter H, Plenk .Jr H ., *Journal of Biomedical Materials Research* 1987,21:881-96
3. A. Samide, C. Negrila, A. Ciuciu ,*Journal of Nanomaterials and Biostructures*, 2010, Vol. 5, No 4,1001-1008
4. A. Adithya Plato Siddharth, *Digest J. Nanomaterials and Biostructures*, **4**, 783 (2009)
5. T. Hanawa, Sci.. *Adv. Mat*.**3**, 289 (2002).
6. T. Hanawa[1,*], K. Asami[2] and K. Asaoka[1] , *Journal of Biomaterials Research* , Article first published online: 6 DEC 1998 DOI: 10.1002/(SICI)1097-4636(19980615)40:4<530::AID-JBM3>3.0.CO;2-G
7. A.Samide, I. Bibicu, B. Oprea, N. Cioatera, A. Ciuciu, J. Optoelectron. *Adv.Mater*.**10**, 1431 (2008).
8. I.Bibicu, A. Samide, B.Oprea, B.Tutunaru, J.Optoelectron. *Adv.Mat*.**10**, 2156 (2008).
9. B.Tutunaru, A. Samide, I. Bibicu, M. Preda, J.Optoelectron. *Adv.Mat*.**11**, 3400 (2007).
10. B. Tutunaru, A. Samide, M. Preda, *Rev. Chim.* **55**, 757 (2004)
11. Daniela T, Dan T , Bogdan O , Adriana S. *Journal of Nanomaterials and Biostructures* , 2013, Vol. 8, No. 1, 35 - 41
12. A. Samid* , C. Negrila , A. Ciucid, *Digest Journal of Nanomaterials and Biostructures* Vol. 5, No 4, October-December 2010, p. 1001-1008
13. T. Hanawa, K. Asami, K. Asaoka, , *Corros. Sci.*, (1996). 38,1579
14. T. Hanawa, K. Asami, K. Asaoka, ,*Corros.Sci*.,(1996),38, 2061
15. Rau´ l Garcı´a Carrodeguas,z,z Antonio H. De Aza,y Xavier Turrillas,J Pilar Penay, and Salvador De Aza, *J. Am. Ceram. Soc*.,(2008), 91 [4], 1281–1286
16. M. J. Buerger, *.Am. Mineral.*, (1948). 33 [3–4], 101–21
17. M. J. Buerger, *Phase Transformations in Solids*, (1951), pp. 183–211
18. Tejpreet Singh, Niraj Bala and Lakhvir Singh, *Int Journal of Surface Engineering & Mater Technol*, (2013), Vol. 3 No. 1,5-9
19. Kean-Khoon Chew, Sharif Hussein Sharif Zein, Abdul Latif Ahmad Natural Science, *International Journal of Advances in Engineering & Technology*, (2012), Vol.4, No.3, 184-188
20. A. Mina, J. C. Caicedo1, W. Aperador, *Int. J.Electrochem. Sci.*, (2013) ,8, 11186 – 11200
21. M. Federica De Riccardis , *Applications in Engineering*, (2012), 44-69

22. Lunguo Xia, Zhiyuan Zhang, Lei Chen, Wenjie Zhang, Deliang Zeng, Xiuli Zhang, Jiang Chang and Xinquan Jiang, ,*European Cell and Materials* ,(2011), 22, *68-83*

23. Christu Tardei, Mariana Spataru, Florentina M. Albu, Stefania Stoleriu, Anghel Ioncea, *Romanian Journal of Materias*, (2013), 43 (1), 41-47

24. Jayanta Kumar Saha, P K Mitra, S Paul & D D N Singh ,*Indian Journal and chemical Technology* , (2010), 17, p 102-110 in